

UNIVERSITY OF
WATERLOO



DEPARTMENT OF MECHANICAL AND MECHATRONICS
ENGINEERING

Title

Author:
James Graham-Hu

Student Number:
20555690

Date: August 31, 2019

August 31, 2019

William Melek, Director
Mechatronics Engineering
University of Waterloo
Waterloo, Ontario
N2L 3G1

Dear Professor Melek,

This report entitled "Title", was prepared as my Work Report 400 for the Department of Mechanical and Mechatronics Engineering at the University of Waterloo for the 4A term. Purpose of report.

Description of Amii.

Description of project and motivation behind project.

Thank you. This report was written entirely by me and has not received any previous academic credit at this or any other institution.

Sincerely,

James Graham-Hu
ID 20555690
4A Mechatronics Engineering

Contents

1	Summary	1
2	Introduction	2
2.1	Problem Definition	2
2.2	Objective	2
3	Background	2
3.1	Automatic Levelling Wrist Background	2
3.1.1	Automatic Levelling Method	4
3.2	Neural Network Background	6
3.2.1	Backpropagation	6
3.2.2	Levenberg-Marquardt Algorithm	7
3.2.3	Numerically Calculating the Jacobian of the Servo	7
4	Proposed Solutions	8
4.1	Criteria and Constraints	8
4.2	Neural Network Methods	9
4.2.1	PID Auto-Tuning, Trained Model-Free using Backpropagation	9
4.2.2	PID Auto-Tuning, Trained Model-Free using the Levenberg-Marquardt Algorithm	11
4.2.3	PID Auto-Tuning, Trained with a Model using the Levenberg-Marquardt Algorithm	11
5	Solution Evaluation	13
5.1	PID Auto-Tuning - Trained with Model, using Levenberg-Marquardt	13
5.2	PID Auto-Tuning - Trained Model-Free, using Levenberg-Marquardt	13

5.3	PID Auto-Tuning - Trained Model-Free, using backpropagation	13
5.4	Chosen Solution	13
6	PID Auto-Tuning Implementation	13
6.1	Servo Transfer Function	14
6.2	Single DOF Simulation	14
6.3	Neural Network Structure	14
6.4	Levenberg-Marquardt Algorithm Implementation	14
6.5	Amplitude Modulated Pseudo-Random Binary Signal (APRBS) Generation .	14
7	Results	16
8	Conclusion	16
9	Recommendations	16
	Appendices	17
A	Appendix	17

List of Figures

1	Automatic levelling of the flexion. The angle, θ , of the flexion servo is constant with the ground as the arm moves (represented by the green dashed line) [4].	3
2	Diagram of the automatic levelling wrist bypass protheses [4].	4
3	Coordinate system and angles, ϕ and θ . The projections of the IMU gravity vector (GV) can be used to calculate ϕ and θ [4].	5
4	Block diagram of the control loop for one servo.	6
5	Block diagram of the training process for the PID neural network using the servo neural network to mimic the actual servo output.	10
6	Block diagram of the training process for the servo neural network.	11
7	Sample figure	15

List of Tables

1	Parameters for the MX-28AT servo model [6]	12
2	Sample table2	14

1 Summary

Summary

2 Introduction

2.1 Problem Definition

Demos can provide an interesting and intuitive way to demonstrate the capabilities and advantages of machine learning to interested parties. Although a few software demos exist at Amii, there is currently no demo that implements machine learning on a hardware system. The advantage of implementing machine learning on hardware is that it is a hands-on way of demonstrating how machine learning can improve a system or be applied to a problem. The problem this project addresses is the lack of a hardware demo to demonstrate machine learning at Amii.

2.2 Objective

The automatic levelling wrist, developed by Dylan A. J. Brenneis as part of his Master's thesis in 2019, [4] is a good candidate for a hardware system that can be improved with machine learning. The objective of this project is to use machine learning to improve the automatic levelling wrist in a meaningful and demonstrable way.

3 Background

3.1 Automatic Levelling Wrist Background

Powered wrist movement is rare in commercial systems, and many powered prostheses have only one degree of freedom (DOF), usually rotation [1]. These limitations in ease of wrist movement in many upper limb prostheses force people with major upper limb loss to use compensatory movements [2]. Compensation occurs with trunk, shoulder, and elbow movements, and has been associated with causing musculoskeletal pain in the neck, upper back, shoulder, and remaining arm [3].

A two DOF automatic levelling wrist was developed by Dylan J. A. Brenneis in 2019 that addresses the issues with ease of wrist movement in wrist prosthetics [4]. The two DOF automatic levelling wrist provides two degrees of freedom, rotation and flexion of the wrist. The user has the ability to switch between controlling the position of the flexion, or letting it automatically level itself to maintain its angle with the ground (see figure 1). The rotation of the wrist is always automatically leveled to be flat with the ground. These features are shown to reduce compensatory movements in vertically-oriented tasks. However, the current implementation of the automatic levelling wrist is reported as unreliable and unintuitive in user tests [4]. Possible reasons for a feeling of unreliability from users could be a result of

slow response time, oscillations, and poor disturbance rejection in the automatic levelling system.

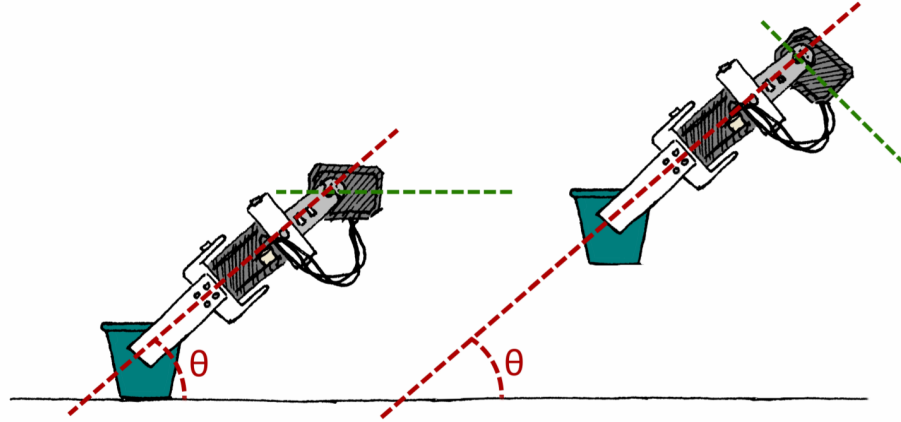


Figure 1: Automatic levelling of the flexion. The angle, θ , of the flexion servo is constant with the ground as the arm moves (represented by the green dashed line) [4].

Figure 2 shows the design of the automatic levelling wrist. Three MX-28AT servos are used to actuate the prosthetic wrist. Two servos provide the degrees of freedom for wrist rotation and flexion, and the third servo is used to manipulate a gripper. It should be noted that the automatic levelling wrist is designed as a bypass protheses so that an able-bodied person is able to use it. A higher statistical power is able to be achieved in a more time efficient way by running trials with able-bodied persons, because of limitations in participant availability when running trials with participants affected by amputation [4].

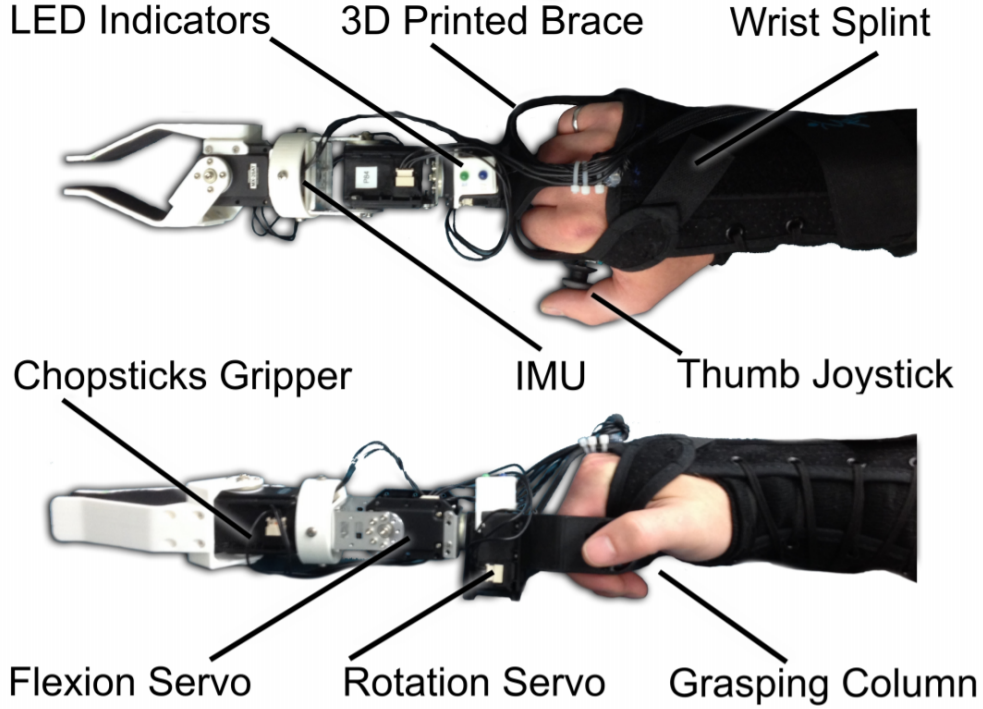


Figure 2: Diagram of the automatic levelling wrist bypass protheses [4].

3.1.1 Automatic Levelling Method

The wrist is automatically leveled using an Adafruit 9-DOF absolute orientation IMU fusion breakout (BNO055) attached to the base of the gripper, as seen in figure 2, and two independent PID controllers, one for the rotation servo and one for the flexion servo. The gravity vector from the IMU is used to calculate the current angle of rotation and flexion. The error between the calculated angle and the setpoint is fed into the PID controller to generate a control signal for the servo. The setpoint for the rotation servo is always set to 180° while the setpoint for the flexion servo is set to where the user last moved it to before switching to automatic levelling. Figure 3 shows the definitions for the coordinate system, the angle of rotation, ϕ , and the angle of flexion, θ .

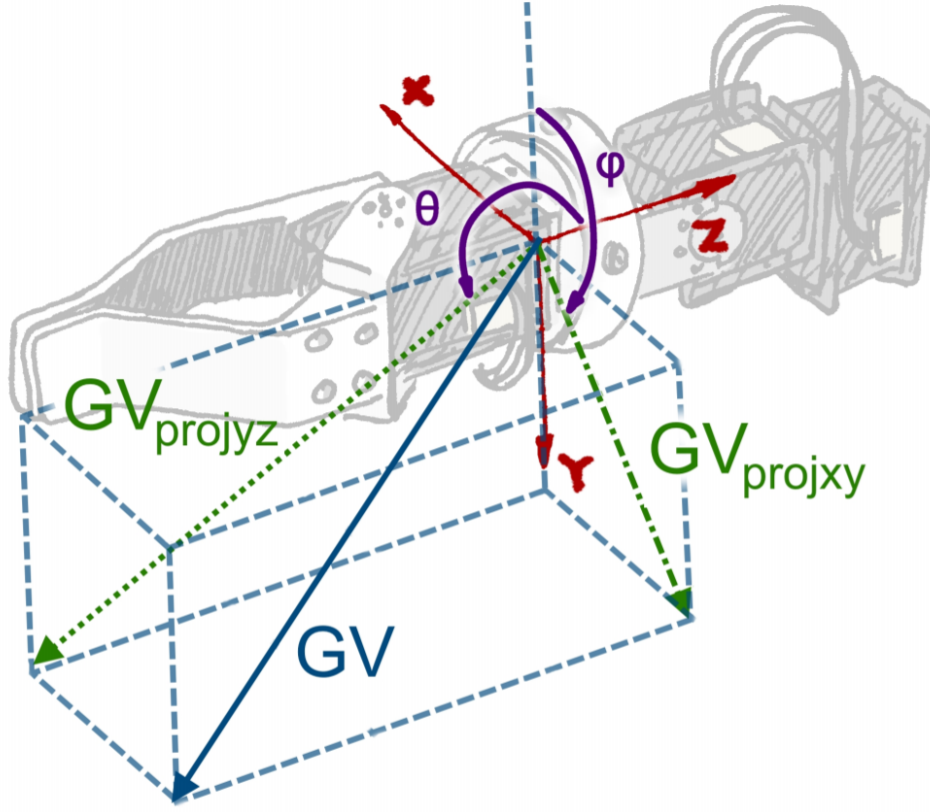


Figure 3: Coordinate system and angles, ϕ and θ . The projections of the IMU gravity vector (GV) can be used to calculate ϕ and θ [4].

ϕ is defined as the angle between the negative y-axis and the projection of the gravity vector in the x-y plane. θ is defined as the angle between the positive z-axis and the projection of the gravity vector projected in the y-z plane.

Figure 4 shows the block diagram for one servo in the automatic levelling wrist. A simple PID control loop controls the position of the servo. The equation for the PID controller signal, $u(t)$, is given by equation 1. The servo position is summed with a disturbance, $d(t)$ which models the angle the wrist is rotated by the user, and fed through the IMU to acquire either ϕ or θ . The block diagram for the rotation and flexion servos are the same other than the K_p , K_i , and K_d gain values for the PID controllers, the IMU function, and the value of the disturbance, $d(t)$. The disturbance is considered as the angle of the user's wrist with respect to a fixed coordinate system that is coincident with the user's wrist when it is completely level with the ground. Note that in the actual implementation of the control loop, the disturbance and servo position aren't directly used. Rather, they are implicitly included when the IMU measures the gravity vector since the gravity vector changes based on the disturbance and servo positions.

$$u(t) = K_p e(t) + K_i \int e(t) dt + K_d \frac{de(t)}{dt} \quad (1)$$

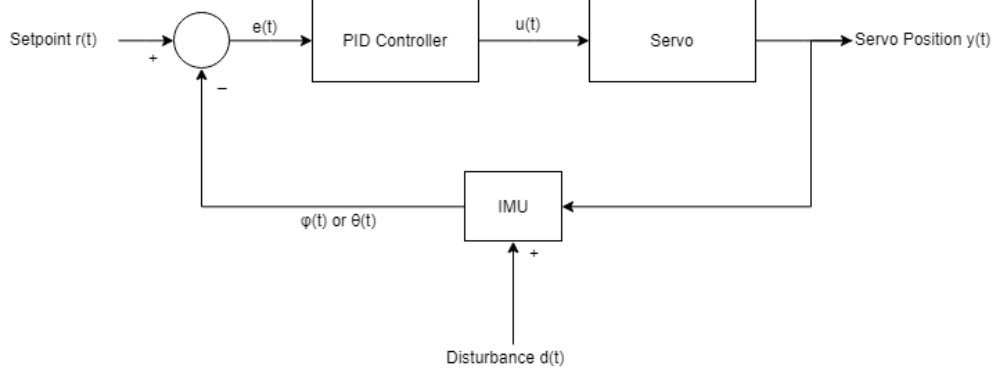


Figure 4: Block diagram of the control loop for one servo.

3.2 Neural Network Background

In machine learning, neural networks are used to represent non-linear functions by making use of one or more hidden layers and activation functions. Figure ?? shows the structure of a neural network with one hidden layer. In this network, the input vector, X , is multiplied by the weight matrix W_0 and summed with the bias vector b_0 . The result of that is then put through an activation function, giving a vector of activations. These activations are then multiplied by the weight matrix W_1 and summed with the bias vector b_1 to give the output, y . The output can also be put through an activation function. In regression, a linear activation function is mostly used on the output. Activation functions used in the hidden layer include but are not limited to the hyperbolic tangent, sigmoid, and rectified linear unit (ReLU) functions. The choice of activation function is dependent on the application of the neural network.

3.2.1 Backpropagation

Learning for a neural network is most commonly accomplished by backpropagation. Backpropagation is performed by calculating the derivative of the squared error of the neural network with respect to each weight in the network. The squared error of the neural network is defined in equation 2. The equation is divided by two to simplify the derivative. Since the entire network including its activation functions is differentiable, the chain rule can be used to backpropagate the error between the neural network's output and what the output should be (the label) back to the weights. Equation 3 is the update function used for weight $w_{i,j}$ in the neural network which updates the weights at a learning rate α .

$$E = \frac{1}{2}(y_{true} - y_{pred})^2 \quad (2)$$

$$w_{i,j} \leftarrow w_{i,j} + \alpha \frac{\partial E}{\partial w_{i,j}} \quad (3)$$

3.2.2 Levenberg-Marquardt Algorithm

Another method for training neural networks is using the Levenberg-Marquardt algorithm. The Levenberg-Marquardt algorithm uses the jacobian of the output with respect to the weights of the neural network to solve for an adjustment for each weight. Equation 4 is solved for σ to determine the adjustments for each weight.

$$[J_w^T J_w + \lambda I] \sigma = J_w^T [E] \quad (4)$$

Here, J_w is the jacobian of the output with respect to the weights, λ is the damping factor, I is the identity matrix, σ is the adjustment matrix, and E is the difference between the outputs and the labels. Isolating for σ yields equation 5. The damping factor, λ , is increased if $[J_w^T J_w + \lambda I]$ is not invertible. Once σ is acquired, it is added to the previous weights to move them closer to the optimal values. This process is repeated iteratively until the weights converge.

$$\sigma = [J_w^T J_w + \lambda I]^{-1} J_w^T [E] \quad (5)$$

For a system, $y(\mathbf{u}_i, \mathbf{w})$ with one output, an input vector, \mathbf{u}_i , n timesteps, and k weights, the jacobian with respect to the neural network weights is expressed as equation 6.

$$J_w = \begin{bmatrix} \frac{\partial y(\mathbf{u}_0, \mathbf{w})}{\partial w_0} & \frac{\partial y(\mathbf{u}_0, \mathbf{w})}{\partial w_1} & \dots & \frac{\partial y(\mathbf{u}_0, \mathbf{w})}{\partial w_k} \\ \frac{\partial y(\mathbf{u}_1, \mathbf{w})}{\partial w_0} & \frac{\partial y(\mathbf{u}_1, \mathbf{w})}{\partial w_1} & \dots & \frac{\partial y(\mathbf{u}_1, \mathbf{w})}{\partial w_k} \\ \vdots & \vdots & \ddots & \vdots \\ \frac{\partial y(\mathbf{u}_n, \mathbf{w})}{\partial w_0} & \frac{\partial y(\mathbf{u}_n, \mathbf{w})}{\partial w_1} & \dots & \frac{\partial y(\mathbf{u}_n, \mathbf{w})}{\partial w_k} \end{bmatrix} \quad (6)$$

3.2.3 Numerically Calculating the Jacobian of the Servo

To numerically calculate jacobian of a servo, each weight is individually changed by a small amount, ϵ and then an input signal is sent to the servo. The change in servo response before and after the small weight change is recorded and used to calculate a finite backward difference to approximate the partial derivative of the system with respect to the weight that

was changed. Equation 7 demonstrates this calculation of the approximate jacobian matrix. The dimension of the resultant jacobian matrix is n rows by k columns.

$$\begin{aligned}
 J_w &= \begin{bmatrix} \frac{\partial \mathbf{y}(\mathbf{u}, \mathbf{w})}{\partial w_0} & \frac{\partial \mathbf{y}(\mathbf{u}, \mathbf{w})}{\partial w_1} & \cdots & \frac{\partial \mathbf{y}(\mathbf{u}, \mathbf{w})}{\partial w_k} \end{bmatrix} \\
 \frac{\partial \mathbf{y}(\mathbf{u}, \mathbf{w})}{\partial w_i} &= \frac{\mathbf{y}(\mathbf{u}, \mathbf{w}) - \mathbf{y}(\mathbf{u}, \mathbf{w} - \mathbf{h}\epsilon(\mathbf{w}_i))}{\epsilon(w_i)} \\
 h_p &= 1, p = i \\
 h_p &= 0, p \neq i
 \end{aligned} \tag{7}$$

4 Proposed Solutions

4.1 Criteria and Constraints

The proposed solutions for the project were constrained according to the following constraints.

- The solution must improve the performance of the automatic levelling wrist.
- The solution must implement machine learning in some way.

The following criteria considered in choosing an appropriate solution are chosen such that the automatic levelling wrist reliably improves the user's ability to use the prosthetic.

- The solution should minimize steady state error.
- The solution should minimize response time.
- The solution should minimize settling time.
- The solution should maximize reliability and consistency.

Due to the nature of the problem, training time and data are difficult to acquire. Without a simulation, data and training can only be collected and run in real time. Therefore, the solution should require minimal training time and data, or be able to make use of a simulation.

4.2 Neural Network Methods

The three neural network methods proposed in this section make use of the PID control loop described in Figure 4. A neural network that outputs the PID gains, K_p , K_i , and K_d is added to the control loop. The neural network takes the error between the setpoint and the current angle of the servo, the current angle of the servo, and the velocity of the servo. The goal is to train the neural network so that it will output appropriate gains for any situation, such that the system has the best response time and error for that situation. The rotation and flexion servos will use separately trained neural networks to output gains for their respective PID controllers. In this section the rotation servo will be used to explain the method, but the same method can be applied to both rotation and flexion servos.

4.2.1 PID Auto-Tuning, Trained Model-Free using Backpropagation

Since no labels exist for the PID gains at the output of the neural network (it is unknown what the gains should be in any given situation) the error term used to train the neural network, E , must be the squared error between the servo angle, $\phi(t)$ and the setpoint, $r(t)$ as shown in equation 8. To train the neural network, this error must be backpropagated through the servo and the PID controller to the neural network output, \mathbf{m} . Performing the chain rule on the partial derivative of E with respect to \mathbf{m} yields 9. This partial derivative can then be backpropagated through the neural network to train the weights.

$$E = \frac{1}{2}(r - \phi)^2 \quad (8)$$

$$\frac{\partial E}{\partial \mathbf{m}} = \begin{bmatrix} \frac{\partial E}{\partial \phi} \frac{\partial \phi}{\partial u} \frac{\partial u}{\partial K_p} \\ \frac{\partial E}{\partial \phi} \frac{\partial \phi}{\partial u} \frac{\partial u}{\partial K_i} \\ \frac{\partial E}{\partial \phi} \frac{\partial \phi}{\partial u} \frac{\partial u}{\partial K_d} \end{bmatrix} \quad (9)$$

Here, ϕ is the rotation servo angle, u is the control signal from the PID controller defined in equation 1, and K_p , K_i , and K_d are the PID gains. The solutions to the individual partial derivatives are shown in equation 10

$$\begin{aligned}
\frac{\partial E}{\partial \phi} &= r - \phi \\
\frac{\partial \phi}{\partial u} &=? \\
\frac{\partial u}{\partial K_p} &= e(t) \\
\frac{\partial u}{\partial K_i} &= \int e(t) dt \\
\frac{\partial u}{\partial K_d} &= \frac{de(t)}{dt}
\end{aligned} \tag{10}$$

Since the time domain function of the servo, $\phi(t)$ is not known, it is not possible to solve for $\frac{\partial \phi}{\partial u}$. To address this problem, a second neural network that mimics the servo is used to output the servo angle rather than the actual servo. This allows the error to be backpropagated through the neural network, through the PID controller and to the PID neural network. Figure 5 is the control loop block diagram with the added PID neural network and servo neural network. The servo neural network will be trained on the actual response of the servo. By treating the input to the servo as the input to the neural network, and the output of the servo as the labels for training, backpropagation can be performed to train the servo neural network on a dataset of inputs and outputs given by the actual servo. Figure 6 demonstrates the training process for the servo neural network. Once trained, the servo neural network is implemented into the control loop to train the PID neural network using backpropagation. After training the PID neural network, the PID neural network is implemented into the actual system.

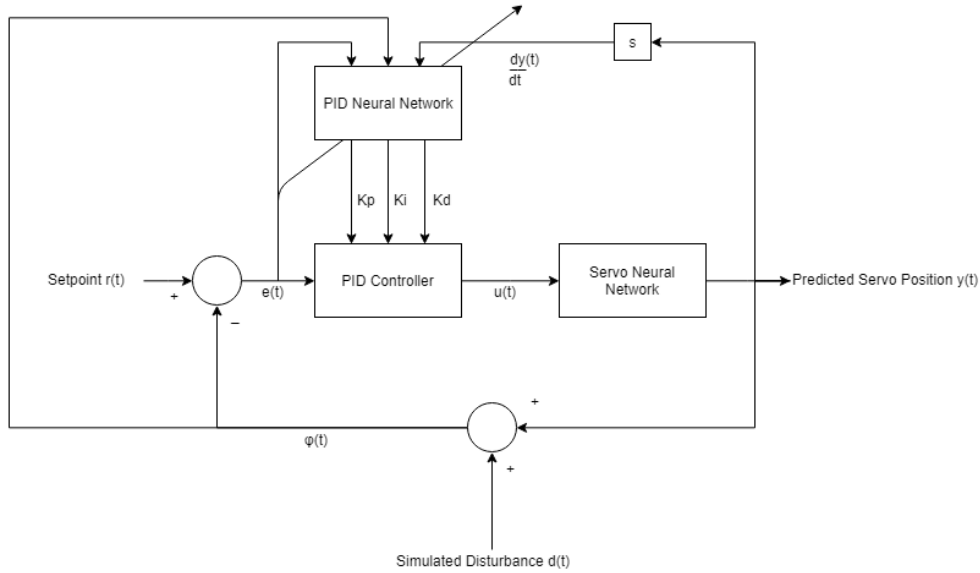


Figure 5: Block diagram of the training process for the PID neural network using the servo neural network to mimic the actual servo output.

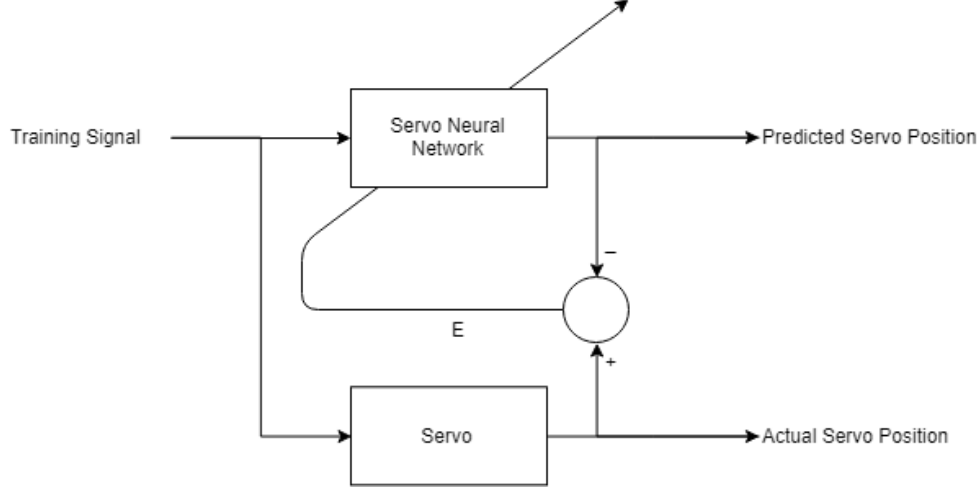


Figure 6: Block diagram of the training process for the servo neural network.

4.2.2 PID Auto-Tuning, Trained Model-Free using the Levenberg-Marquardt Algorithm

Rather than using backpropagation to train the weights of the PID neural network, the Levenberg-Marquardt algorithm is used to train the PID neural network as described in section 3.2.2. Equation 11 is used to solve for the weight adjustments, σ , using the difference between the servo angle, ϕ , and the setpoint, r , as the error term. A servo neural network, trained the same way as described in 4.2.1 is used to simulate the servo response to small weight changes needed to calculate the jacobian of the servo outlined in section 3.2.3.

$$\sigma = [J_w^T J_w + \lambda I]^{-1} J_w^T [\phi - r] \quad (11)$$

4.2.3 PID Auto-Tuning, Trained with a Model using the Levenberg-Marquardt Algorithm

Similar to section 4.2.2 this method uses the Levenberg-Marquardt algorithm to train the PID neural network. However, when numerically calculating the jacobian, rather than using a neural network to simulate the servo response to small weight changes, a mathematical model of the servo is used. Equation 12 is the simplified transfer function of the servo, assuming the electrical dynamics of the servo are much faster than the mechanical dynamics [6].

$$\frac{Y(s)}{U(s)} = \frac{N\eta K_t (K_d s^2 + K_p s + K_i)}{R(J_l + J_m N^2 \eta) s^3 + (b_m N^2 \eta R + \frac{K_t N^2 \eta}{K_w} + N\eta K_t K_d) s^2 + N\eta K_t K_p s + N\eta K_t K_i} \quad (12)$$

Here, $Y(s)$ is the laplace transform of the servo angle, $U(s)$ is the laplace transform of the input signal. The MX-28AT servo contains an internal PID controller with internal gains. Since the servo is controlled in ticks rather than radians, the gains must be converted so that they can be used in the transfer function which is in radians. Equation 13 shows the conversion process.

$$\begin{aligned} K_p &= \frac{P}{8} \frac{2048 V_s}{511\pi} \\ K_i &= \frac{1000 I}{2048} \frac{2048 V_s}{511\pi} \\ K_d &= \frac{4 D}{1000} \frac{2048 V_s}{511\pi} \end{aligned} \quad (13)$$

Here, V_s is the source voltage which is 12V, and P , I , and D are gains set by the user, which are $P = 32$, $I = 0$, and $D = 0$ by default. The user manual for the MX-28AT also states that the gains set by the user must be converted to get their values in ticks, hence the multiplication by $\frac{1}{8}$, $\frac{1000}{2048}$ and $\frac{4}{1000}$ for P , I , and D respectively [7].

The load inertia, J_l , depends on the servo. For the rotation servo the inertia is estimated as the inertia of a rectangular prism, which represents the flexion servo, rotating on its center axis, and a point mass, which represents the gripper, whose position above the axis of rotation depends on the angle of the flexion servo. For the flexion servo the inertia is estimated as the inertia of a rectangular prism, which represents the gripper, rotating around an axis offset from its center by half its length and the length of the bracket attaching the gripper to the flexion servo. The inertia calculations are shown in equation ??.

The other parameters for equation 12 are described in table 1.

Table 1: Parameters for the MX-28AT servo model [6]

Parameter	Symbol	Value
Motor resistance	R	8.3Ω
Motor gear ratio	N	193
Motor gear efficiency	η	0.836
Speed constant	K_ω	$93.1\text{rad}/V$
Torque constant	K_t	$0.0107\text{Nm}/A$
Motor inertia	J_m	$8.68 \times 10^{-8}\text{kgm}^2$
Friction	b_m	$8.87 \times 10^{-8}\text{Nm s}$

5 Solution Evaluation

5.1 PID Auto-Tuning - Trained with Model, using Levenberg-Marquardt

Requires a simulation for the servo, however the level of sophistication for the simulation does not need to be extremely high as in an RL setting. Uses a PID controller (so not starting from scratch) which makes it more reliable, as the PID controller on its own will achieve the objective of automatic levelling to a certain level. Therefore a simple simulation can be a starting point. Quick training for the neural network, as a simulation can tune the neural network many times faster than real time.

5.2 PID Auto-Tuning - Trained Model-Free, using Levenberg-Marquardt

Quick training for the neural network, as a simulation can tune the neural network many times faster than real time. However, another neural network must be trained to emulate the real system which requires real data. It was found that there was not enough real data to generalize to all situations. (generalizes well to what it saw, but not anything else like the APRBS used to find the jacobian)

5.3 PID Auto-Tuning - Trained Model-Free, using backpropagation

Same problems as above, as well as being difficult to implement, due to the statefulness of the PID controller.

5.4 Chosen Solution

The chosen solution was PID auto-tuning trained using a model, using the Levenberg-Marquardt algorithm.

6 PID Auto-Tuning Implementation

Required components: a transfer function or ode for the servo, a simulation, a neural network, a numerical implementation of the levenberg marquardt algorithm, a numerical jacobian

calculator, an APRBS generator, a neural network implemented in C#

6.1 Servo Transfer Function

6.2 Single DOF Simulation

Best parameters for simulation

6.3 Neural Network Structure

5 inputs (error, angle, velocity), 4 nodes in hidden layer, 3 output nodes, leaky relu with $\alpha=0.3$ activation function. Absolute value of output to keep positive (can't have negative gains)

6.4 Levenberg-Marquardt Algorithm Implementation

6.5 Amplitude Modulated Pseudo-Random Binary Signal (APRBS) Generation

Table 2: Sample table2

Requests/Second	Required Size	Cores	Memory (GiB)	Cost (\$/month)
10	t2.small	1	2	16.56
100	t2.medium	2	4	33.41
1000	t2.large	2	8	66.82
10000	t2.xlarge	4	16	133.63

$$\text{Sampleequation} \tag{14}$$

UNIVERSITY OF **WATERLOO**



Figure 7: Sample figure

7 Results

8 Conclusion

9 Recommendations

Better Simulation (2 DOF, better approximation of moment of inertia for different servo positions, take torque due to gravity into account)

References

- [1] N. M. Bajaj, A. J. Spiers, and A. M. Dollar, “State of the art in prosthetic wrists: Commercial and research devices”, in *2015 IEEE International Conference on Rehabilitation Robotics (ICORR)*, Aug. 2015, pp. 331–338.
- [2] S. L. Carey, M. J. Highsmith, M. E. Maitland, and R. V. Dubey, “Compensatory movements of transradial prosthesis users during common tasks”, *Clinical Biomechanics*, vol. 23, no. 9, pp. 1128 –1135, 2008.
- [3] K. Østlie, R. J. Franklin, O. H. Skjeldal, A. Skrondal, and P. Magnus, “Musculoskeletal pain and overuse syndromes in adult acquired major upper-limb amputees”, *Archives of Physical Medicine and Rehabilitation*, vol. 92, no. 12, pp. 1967 –1973, 2011.
- [4] D. J. A. Brenneis, ”Automatic Levelling of a Prosthetic Wrist”, *University of Alberta*, 2019.
- [5] R. S. Sutton and A. G. Barto, ”Introduction to reinforcement learning”, *Cambridge: MIT Press*, second edition, 2018.
- [6] M. R. O. A. Maximo, C. H. C. Ribeiro and R. J. M. Afonso, ”Modeling of a position servo used in robotics applications”, *Autonomous Computational Systems Lab (LAB-SCA) and Electronic Engineering Division, Computer Science Division, Aeronautics Institute of Technology, Praça Marechal Eduardo Gomes*, 2017.
- [7] ”Robotis e-manual”, *Robotis*, 2019. [Online]. Available: <http://emanual.robotis.com/docs/en/dxl/mx/mx-28/>. [Accessed: 16-Jul-2019].

Appendices

A Appendix